ChemPubSoc Europe

DOI: 10.1002/chem.201405110

CHEMISTRY
A European Journal
Full Paper

Porphyrinoids

Nucleophilic Aromatic Substitution Reactions of *meso*-Bromosubporphyrin: Synthesis of a Thiopyrane-Fused Subporphyrin

Daiki Shimizu,[a] Hirotaka Mori,[a] Masaaki Kitano,[a] Won-Young Cha,[b] Juwon Oh,[b] Takayuki Tanaka,[a] Dongho Kim,*[b] and Atsuhiro Osuka*[a]

Abstract: *meso*-Bromosubporphyrin undergoes nucleophilic aromatic substitution (S_NAr) reactions with arylamines, diarylamines, phenols, ethanol, thiophenols, and *n*-butanethiol in the presence of suitable bases to provide the corresponding substitution products. The S_NAr reactions also proceed well with pyrrole, indole, and carbazole to provide substitution products in moderate to good yields. Finally, the S_NAr reaction with 2-bromothiophenol and subsequent intramolecular peripheral arylation reaction affords a thiopyrane-fused subporphyrin.

Introduction

Ring-contracted porphyrinoids have attracted considerable attention in recent years as new functional pigments.[1,2] Among these species, subporphyrin is a new and tantalizing addition to porphyrinoid chemistry since it corresponds to analogues of porphyrin missing one pyrrole unit, and features high structural similarity to porphyrins. Since the first synthesis of tribenzosubporphine in 2006,[3] various subporphyrins have been explored for their attractive optical and electronic properties.[3–5] Through these studies, it has been shown that subporphyrins possess properties analogous to porphyrins, such as strong aromaticity and fluorescence emission, but display unique characteristic properties such as bowl-shaped structures and large influences of *meso*-aryl substituents due to facile rotation.[5] Considering the great promise of subporphyrins as functional molecules, new synthetic methods that can be used for fabrication of subporphyrins are highly desired.

meso-Bromosubporphyrin **2a** was synthesized as a useful precursor by bromination of *meso*-substituent-free subporphyrin **1** with *N*-bromosuccinimide (NBS).[6] Pd-catalyzed cross-coupling reactions of **2a** gave A_2B-type subporphyrins bearing various *meso*-substituents including alkynyl, alkenyl, benzyl, aryl, arylamino, arylsulfanyl, aryloxy, ethoxy, and phosphoryl groups.[6,7] In addition, reductive dimerization of **2a** proceeded well with $[Ni(cod)_3]$ (cod=cyclooctadienyl) catalysis to afford a *meso–meso* linked subporphyrin dimer.[8] Despite this progress, catalyst-free nucleophilic aromatic substitution (S_NAr) reactions of subporphyrins have to date not been explored.

In porphyrin chemistry, a few examples of S_NAr reactions were reported by Dolphin[9] and Crossley in the 1980s.[10] In recent years, S_NAr reactions of porphyrins have been reported for specific combinations of halogenated porphyrin substrates and nucleophiles.[11] Quite recently, a more general method for *meso*-functionalization of porphyrin by catalyst-free S_NAr reactions was developed by using Cs_2CO_3 as a base and DMF as a solvent.[12] These successful reactions prompted us to examine catalyst-free S_NAr reactions of **2a** and *meso*-chlorosubporphyrin **2b**. As discussed below, S_NAr reactions of **2a** with various nucleophiles proceeded smoothly without a Pd catalyst.

Results and Discussion

meso-Bromosubporphyrin **2a** was prepared according to the reported method,[6] and *meso*-chlorosubporphyrin **2b** was obtained by treatment of **1** with an equimolar amount of *N*-chlorosuccinimide (NCS) at 60 °C for 12 h in 60% yield (Scheme 1).

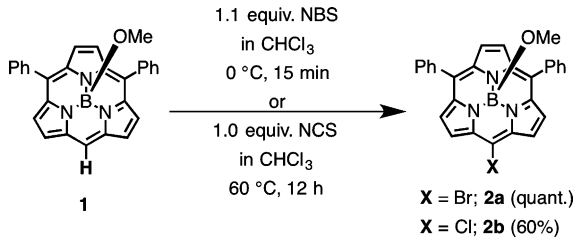

Scheme 1. *meso*-Halogenation reactions of **1**.

[a] D. Shimizu, H. Mori, M. Kitano, Dr. T. Tanaka, Prof. Dr. A. Osuka
Department of Chemistry, Graduate School of Science
Kyoto University, Sakyo-ku, Kyoto 606-8502 (Japan)
E-mail: osuka@kuchem.kyoto-u.ac.jp

[b] W.-Y. Cha, J. Oh, Prof. Dr. D. Kim
Spectroscopy Laboratory for Functional π-Electronic Systems and
Department of Chemistry, Yonsei University, Seoul 120-749 (Korea)
E-mail: dongho@yonsei.ac.kr

Supporting information for this article is available on the WWW under http://dx.doi.org/10.1002/chem.201405110.

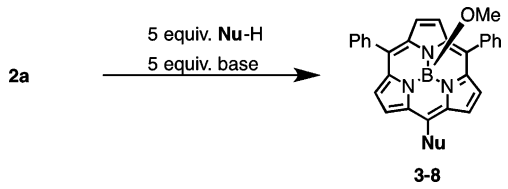

Scheme 2. S_NAr reactions of *meso*-bromosubporphyrin **2a** (see Table 1).

Pd-catalyzed substitution reactions of **2a** with anilines, morpholine, thiophenols, *n*-butanethiol, and phenols proceeded to give the corresponding substitution products (Scheme 2 and Table 1).[7a,c] Catalyst-free S_NAr reaction of **2a** with aniline was started by addition of 1,4-dioxane as a solvent to subporphyrin **2a**, potassium *tert*-butoxide, and aniline placed inside a Schlenk tube at room temperature. The color of the reaction mixture immediately became dark blue. Monitoring the progress of the reaction by TLC indicated that the starting materials were completely consumed after 10 min. Aqueous work-up and subsequent separation by silica gel column chromatography gave *meso*-phenylamino subporphyrin **3a** in 73% yield as a red solid. Since **3a** was strongly adsorbed on silica gel, methanol (1%) was added to an eluent mixture consisting of hexane (50%), CH_2Cl_2 (25%), and ether (25%) to facilitate the elution of **3a**. Whereas the reaction of **2a** with 4-dimethylaminoaniline proceeded rapidly to give **3b** (Table 1, run 2), electron-deficient 4-nitroaniline was unreactive under similar conditions and **3c** was obtained in 35% yield under harsher reaction conditions (Table 1, run 3). Morpholine, an aliphatic amine, gave a complex mixture and **4** was not detected for catalyst-free substitution reactions (Table 1, run 4), while it reacted with **2a** in the Pd-catalyzed reaction to give product **4** in a moderate yield. Thiophenols and *n*-butanethiol reacted nicely with **2a** to give the corresponding substitution products under catalyst-free conditions (Table 1, runs 5, 6, and 8). However, the reaction with 4-nitrothiophenol was very slow in dioxane, probably due to its low nucleophilicity. This reaction proceeded smoothly in DMF to give **5c** (Table 1, run 7). Substitution products **7a** and **8** were obtained in good yields in the reactions of **2a** with phenol and ethanol under catalyst-free conditions (Table 1, runs 9 and 12) but only trace amounts of substitution products were obtained in the reactions of 4-dimethylaminophenol and 4-nitrophenol, due largely to the poor solubilities of their conjugated bases in dioxane. Therefore, these reactions were run in DMF, giving **7b** and **7c** (Table 1, runs 10 and 11), while harsher conditions were required for the reaction with 4-nitrophenol.

Table 2. Results of S_NAr reaction with diarylamines and N-heteroarenes.

Run	Nucleophile	X[a]	Solvent	T [°C]	t	Yield [%][b]
1	Ph_2NH	5	dioxane	25	10 min	72
2	$(4\text{-}MeOC_6H_4)_2NH$	5	dioxane	25	5 min	80
3	$(4\text{-}Me_2NC_6H_4)_2NH$	4	dioxane	25	10 min	46
4	$(4\text{-}O_2NC_6H_4)_2NH$	5	dioxane	25	3 h	n.d.
5	$(4\text{-}O_2NC_6H_4)_2NH$	10	DMF	100	6 h	n.d.
6	$(4\text{-}O_2NC_6H_4)_2NH$	10	DMSO	180	3 h	n.d.
7	$(4\text{-}O_2NC_6H_4)_2NH$	5	DMF	100	22 h	8[c]
8	$(4\text{-}O_2NC_6H_4)_2NH$	1.5	DMSO	140	24 h	41[c]
9	pyrrole	5	DMF	25	30 min	24[d]
10	indole	5	dioxane	25	2 h	6
11	carbazole	5	dioxane	60	30 min	84

[a] X = equivalents of Nu–H/KO*t*Bu (see Scheme 3). [b] n.d. = not detected. [c] **2b** was used as starting material. [d] NaH was used as a base.

In the next step, we examined the substitution reactions with nucleophiles that were not compatible with the Pd-catalyzed substitution reaction (Table 2, Scheme 3). Diphenylamine and bis(4-dimethylphenyl)amine did not provide the corresponding substitution products under the Pd-catalyzed conditions used for arylamination of **2a**.[7a] Gratifyingly, however, under the catalyst-free conditions, the reaction of **2a** with diphenylamine gave *meso*-diphenylamino subporphyrin **9a** in 72% yield as a red solid (Table 2, run 1). In a similar manner, *meso*-bis(4-methoxyphenyl)amino- and *meso*-bis(4-dimethylaminophenyl)amino-substituted subporphyrins (**9b** and **9c**) were synthesized in 80 and 46% yields, respectively (Table 2, runs 2 and 3). However, bis(4-nitrophenyl)amine did not react under similar conditions (Table 2, run 4), or even harsh conditions (Table 2, runs 5 and 6). These results may be ascribed to

Table 1. Comparison between catalyst-free reaction (this work) and Pd-catalyzed reaction.

			This work					Pd-catalyzed reactions					
Run	Nucleophile	Product	Base	Solvent	T [°C]	t	Yield [%]	Catalyst[a]	Base	Solvent	T [°C]	t	Yield [%]
1	Ph-NH_2	**3a**	KO*t*Bu	dioxane	RT	10 min	73	**A**	Cs_2CO_3	THF	reflux	12 h	72[7a]
2	4-$Me_2NC_6H_4$-NH_2	**3b**	KO*t*Bu	dioxane	RT	1 h	82	**A**	Cs_2CO_3	THF	reflux	12 h	64[7a]
3	4-$O_2NC_6H_4$-NH_2	**3c**	KO*t*Bu	dioxane	80	12 h	35	**A**	Cs_2CO_3	THF	reflux	12 h	78[7a]
4	morpholine	**4**	KO*t*Bu	dioxane	RT	10 min	full conv. n.d.	**B**	Cs_2CO_3	THF	reflux	12 h	66[7a]
5	Ph-SH	**5a**	Cs_2CO_3	dioxane	RT	10 h	82	**B**	Cs_2CO_3	toluene	40	30 h	97[7c]
6	4-$Me_2NC_6H_4$-SH	**5b**	Cs_2CO_3	dioxane	RT	12 h	94	**B**	Cs_2CO_3	toluene	40	48 h	92[7c]
7	4-$O_2NC_6H_4$-SH	**5c**	Cs_2CO_3	DMF	RT	1 h	73	**B**	Cs_2CO_3	toluene	40	12 h	89[7c]
8	*n*Bu-SH	**6**	Cs_2CO_3	dioxane	RT	6 h	89	**B**	Cs_2CO_3	toluene	40	12 h	94[7c]
9	Ph-OH	**7a**	Cs_2CO_3	dioxane	60	12 h	87	**B**	KOH	toluene	RT	24 h	76[7c]
10	4-$Me_2NC_6H_4$-OH	**7b**	Cs_2CO_3	DMF	80	12 h	89	**B**	KOH	DMF	80	12 h	86[7c]
11	4-$O_2NC_6H_4$-OH	**7c**	Cs_2CO_3	DMF	150	10 h	49[b]	—	—	—	—	—	—[c]
12	EtONa	**8**	EtONa	dioxane	RT	24 h	73	**B**	EtONa	dioxane	80	24 h	94[7c]

[a] **A** = $Pd(OAc)_2$, DPEphos; **B** = Pd-PEPPSI-IPent. [b] 12 equivalents of nucleophile were used. [c] no reaction was observed.

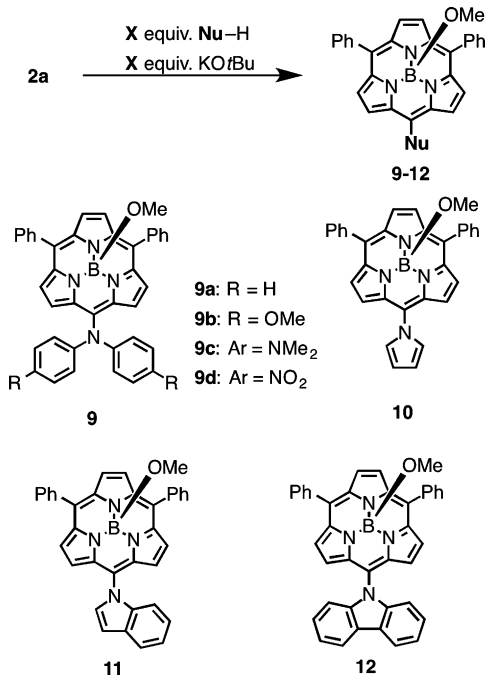

Scheme 3. S_NAr reactions of **2a** with diarylamines and heteroarenes (see Table 2).

low nucleophilicity of bis(4-nitrophenyl)amine. Then, we examined the use of *meso*-chlorosubporphyrin **2b** as a substrate because of its higher reactivity in S_NAr-type reactions. Substitution product **9d** was indeed obtained in 8% yield in the reaction in DMF at 90 °C (Table 2, run 7). Since this reaction was slow and separation of **9d** from the starting amine was tedious, we changed the reaction conditions (Table 2, run 8; the amount of the amine was reduced, DMSO was used as a solvent, and the reaction temperature was increased to 140 °C), which gave **9d** in 41% yield. Product **9d** was not strongly adsorbed onto silica gel, reflecting the poor electron-donating nature of the *meso*-diarylamino substituent. The observed result that **2b** is more reactive than **2a** supports the S_NAr mechanism. High-resolution atmospheric pressure chemical ionization time-of-flight (HR-APCI-TOF) mass spectrometry of newly synthesized subporphyrins **9a**–**d** revealed intense borenium cation peaks at *m/z* 561.2258 $[\mathbf{9a}-OCH_3]^+$, 621.2422 $[\mathbf{9b}-OCH_3]^+$, 647.3089 $[\mathbf{9c}-OCH_3]^+$, and 651.1960 $[\mathbf{9d}-OCH_3]^+$, respectively.

The *N*-containing heteroarenes such as pyrrole, indole, and carbazole also reacted with **2a** under similar conditions to give the corresponding substitution products **10**, **11**, and **12** in 24%, 66%, and 84% yield, respectively. These subporphyrins were less strongly adsorbed onto silica gel in comparison to **9a**. A combination of NaH and DMF was found to shorten the reaction time of **2a** with pyrrole. Nevertheless, the yield of **10** was only modest, probably owing to its chemical instability in solution. In reactions of **2a** with indole or carbazole (Table 2, runs 10 and 11), we used the reaction conditions used for diphenylamine (Table 2, run 1). Substitution products **10**, **11**, and **12** were stable in the solid states. The HR-APCI-TOF mass spectrometry revealed an intense borenium cation peak at *m/z* 459.1779 $[\mathbf{10}-OCH_3]^+$, 509.1945 $[\mathbf{11}-OCH_3]^+$, and 590.2282 $[\mathbf{12}]^+$, respectively. Although several carbazole-appended porphyrins have been recently reported,[13] pyrrole and indole-substituted porphyrinoids have not to date been reported.

In the ^1H NMR spectra of **9a**–**d** taken at room temperature, signals due to the aromatic protons of the diarylamino moieties are observed as a single set, indicating that rotation of the *meso*-arylamino group is faster than the ^1H NMR timescale (Figure 1a). The ^1H NMR spectrum of pyrrole-appended subporphyrin **10** at room temperature exhibits a simple spectral pattern (Figure 1b), which also indicates a faster rotation of the *meso*-pyrrolyl substituent in comparison to the ^1H NMR timescale. In contrast, the ^1H NMR spectrum of indole-appended subporphyrin **11** is rather broad at room temperature, suggesting a restricted rotation of the *meso*-indolyl substituent, which has been confirmed by variable-temperature ^1H NMR measurements. Namely, two rotational isomers are observed as two sets of separate and sharp signals in the ^1H NMR spectrum at

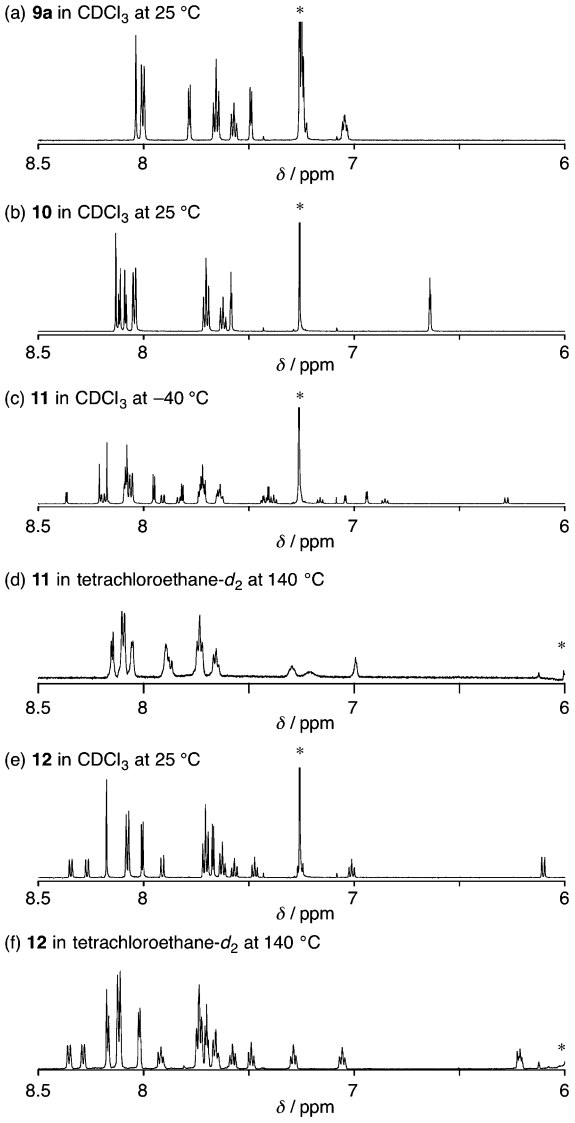

Figure 1. ^1H NMR spectra of **9a** (a), **10** (b), **11** (c, d), and **12** (e, f) under various conditions. * indicates residual solvents.

−40 °C (Figure 1c), which become almost coalesced at 140 °C (Figure 1d). The axial OCH_3 protons are also observed separately as two singlets at 1.00 and 0.89 ppm with a ratio of 3:2, which also coalesced at 140 °C (see the Supporting Information). The ^{1}H NMR spectrum of carbazole-appended subporphyrin **12** is sharp both at room temperature and 140 °C (Figure 1e and f), featuring different signals for the protons of the carbazole located at the exo and endo sides of the subporphyrins, clearly indicating a strictly prohibited rotation of the *meso*-carbazole substituent with a high activation barrier.

The structures of **9a–c**, **10**, **11**, and **12** have been confirmed by single-crystal X-ray diffraction analysis (Figure 2). Similarly to

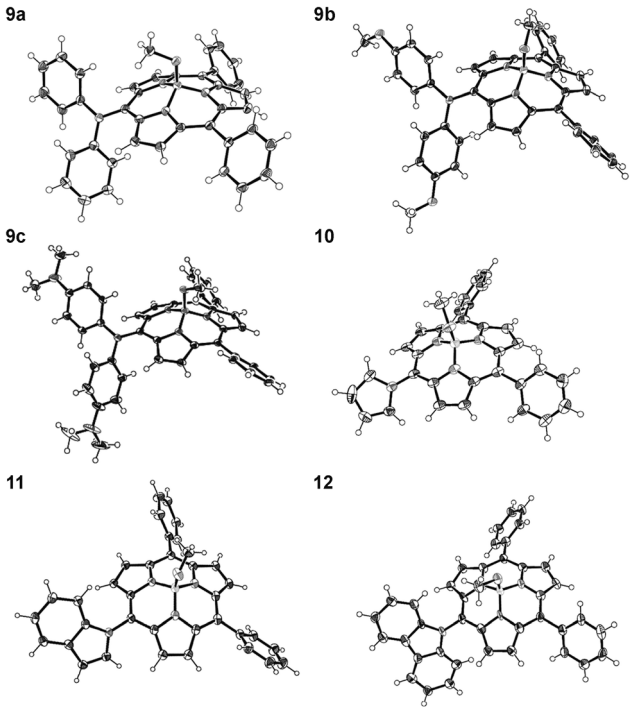

Figure 2. X-ray crystal structures of **9a–c**, **10**, **11**, and **12**. Thermal ellipsoids are set at 50% probability level. Solvent molecules are omitted for clarity.

meso-arylamino-substituted subporphyrins **3a** and **3b**, **9a–c** exhibit C_{meso}–N bond lengths that are distinctly shorter than C_{ipso}–N bond lengths (see the Supporting Information), suggesting the double-bond character of the C_{meso}–N bonds that becomes increasingly significant in the order of **9a** < **9b** < **9c**. Curiously, the two C_{ipso}–N bond lengths are different in **9a–c**. The C_{ipso}–N bonds at the convex side are always slightly longer than those at the concave side in the crystals. The nitrogen atoms attached at the *meso* position show planar trivalent coordination, as revealed by the sum of the angles around the nitrogen atoms of **9a–c**; 360°, 358°, and 359°, respectively. Dihedral angles of the diarylamino-substituents towards the subporphyrin cores are lying in the range of 42-47°. Different from **9a–c**, subporphyrins **10–12** display longer C_{meso}–N bonds (see the Supporting Information), suggesting much weaker or negligible electron-pair donating interactions of the *meso*-substituents.

The UV/Vis absorption and fluorescence spectra of **9a–d** and **10–12** are shown in Figure 3 (a and b), along with those of *meso*-phenylamino subporphyrin **3a** and *meso*-triphenyl subporphyrin **13**. The relevant data are listed in Table 3. Electronic properties of subporphyrins are largely perturbed by the electron-donating characters of *meso*-diarylamino substituents. Therefore, it is natural to observe stronger influences for more electron-rich *meso*-diarylamino substituents. Large perturbations of the electronic properties of subporphyrins are ob-

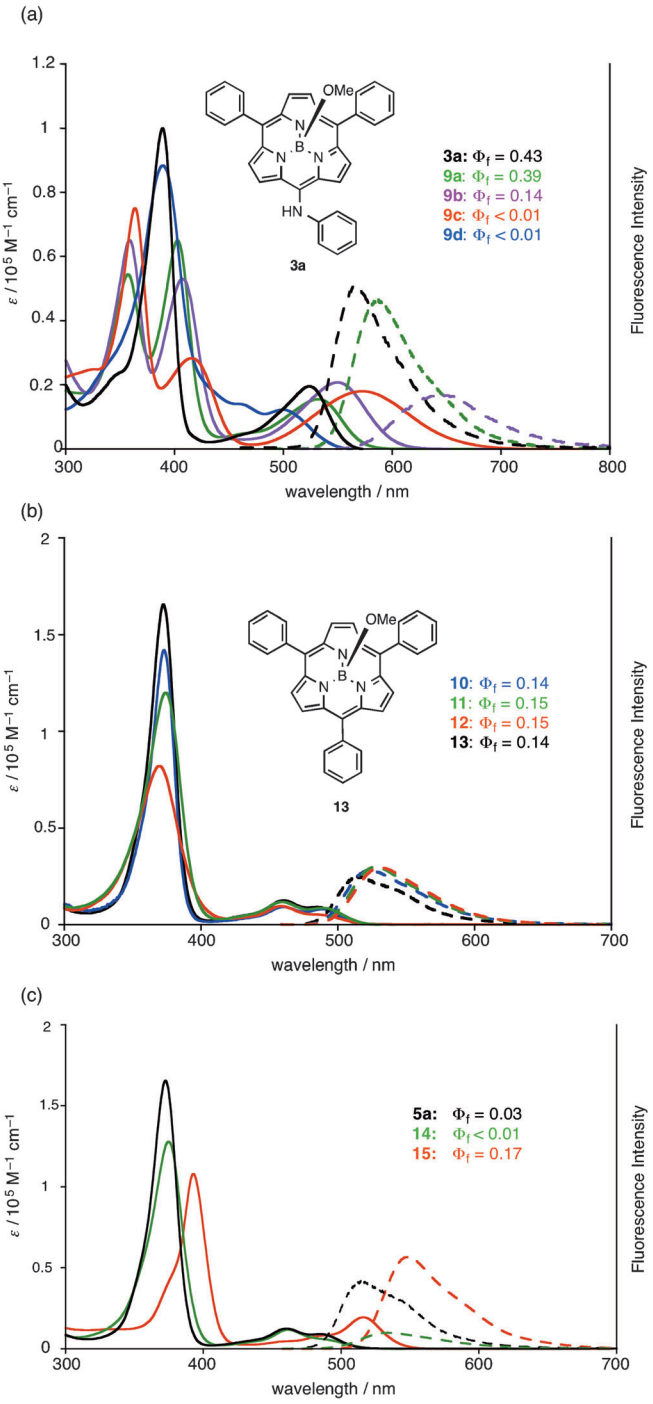

Figure 3. UV/Vis absorption (solid) and fluorescence (dashed) spectra of a) **3a** and **9a–d**, b) **10**, **11**, **12**, and **13**, and c) **5**, **14**, and **15**.

Table 3. Optical properties of subporphyrins **9a–d** and **10–15**.

	λ_{abs} [nm] (ε [$M^{-1}cm^{-1}$])	λ_{em} [nm]	Φ_F[b]
9a	357 (54000), 403 (65000), 530 (15000)	587	0.39
9b	359 (65000), 408 (53000), 553 (21000)	643	0.14
9c	364 (75000), 415 (28000), 574 (18000)	—	<0.01
9d	390 (88000), 501 (12000)	—	<0.01
10	373 (142000), 459 (9000), 489 (8000)	523	0.14
11	374 (120000), 459 (12000), 489 (9000)	528	0.15
12	376 (111000), 459 (10000), 483 (5000)	531	0.15
13	373 (166000), 461(13000), 484(9000)	516	0.14
14	375 (120000), 461 (11000)	—	<0.01
15	394 (108000), 516 (20000)	548	0.17

[a] Measured in CH_2Cl_2. [b] Fluorescence quantum yield.

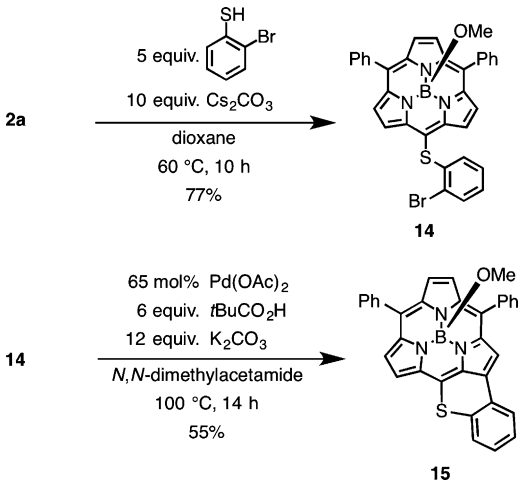

Scheme 4. Synthesis of thiopyrane-fused subporphyrin **15.**

served in the absorption spectra of **9a–d**; a Soret-like band is remarkably split into two bands at 357 and 403 nm for **9a**, at 359 and 408 nm for **9b**, and at 364 and 415 nm for **9c**. Such band splitting was detected only for **3b** among the arylamino subporphyrins, whose splitting width was smaller than those of **9a–c**. In going from **9a**→**9b**→**9c**, the high-energy split bands are increasingly intensified at the expense of the low-energy split bands, and the Q-like bands are steadily red-shifted in this order. In contrast, the absorption spectrum of *meso*-bis(4-nitrophenyl)amino-substituted subporphyrin **9d** shows a non-split broad Soret-like band at 390 nm and its Q-like band is blue-shifted in comparison to **13**. Subporphyrins **9a** and **9b** show fluorescence spectra at 587 and 643 nm, which are distinctly red-shifted in comparison to that of **13**, but subporphyrins **9c** and **9d** are virtually non-fluorescent. Fluorescence quantum yields of **9a** and **9b** were determined by a sphere-type digital photon-counting instrument to be 0.388 and 0.143, respectively. Observed efficient fluorescence quenching in **9c** and **9d** has been accounted for in terms of intramolecular electron transfer, in a manner similar to previously reported *meso*-arylaminosubporphyrins.[7b]

Pyrrole-, indole-, and carbazole-appended subporphyrins **10**, **11**, and **12** display Soret-like and Q-like bands, which are roughly analogous to those of **13**, while band broadening of Soret-like band becomes prominent in the order of **10**<**11**<**12**. Fluorescence quantum yields were determined to be 0.14, 0.15, and 0.15 for **10**, **11**, and **12**, respectively, which are also quite similar to that of **13** (0.14). Fluorescence lifetimes in toluene have been determined by time-correlated single photon counting (TCSPC) methods to be 2.4, 2.5, and 2.6 ns for **10**, **11**, and **12**, respectively, again being similar to that of **13** (2.8 ns). These results indicate that these pyrrolic heterocycles do not serve as an electron donor towards the directly linked subporphyrin chromophore.

Finally, we attempted to prepare a subporphyrin bearing an externally fused aromatic segment on the basis of the S_NAr reaction. The synthetic route is outlined in Scheme 4, in which the S_NAr reaction of **2a** with 2-bromothiophenol afforded substitution product **14**, which was fused by an intramolecular C–H activation reaction to give fused subporphyrin **15**. A key idea behind this plan is that 2-bromothiophenol will work as a nucleophile in the S_NAr reaction of **2a** to produce a substitution product bearing a *meso*-2-bromophenylsulfanyl substituent, since **2a** is a much more reactive substrate for the S_NAr reaction than 2-bromothiophenol. As expected, the reaction of **2a** with 2-bromothiophenol proceeded rapidly to produce 2-bromophenylsulfanyl subporphyrin **14** in 77% yield. Its HR-APCI-TOF mass spectrum revealed a borenium cation peak at *m/z* 580.0659 [**14**–OCH_3]$^+$, and its ^{1}H NMR spectrum indicated the protons of the (2-bromophenyl)sulfanyl group at 7.62, 6.93, 6.86, and 6.45 ppm, respectively. An intramolecular fusion reaction of **14** was effected by subjecting it to reaction conditions that were used for Pd-catalyzed direct arylation at the β-position of *meso*-substituent-free Ni^{II}–porphyrins [$Pd(OAc)_2$ (65 mol%), *tert*-$BuCO_2H$ (6 equiv), K_2CO_3 (12 equiv) in *N*,*N*-dimethylacetamide (DMA) at 100 °C, 14 h].[14] After the usual work-up, thiopyrane-fused subporphyrin **15** was isolated as a red solid in 55% yield. **15** is a rare example of a subporphyrin bearing an externally fused aromatic entity. Only one example has been reported for such fused subporphyrins.[4d] The parent ion peak of **15** was detected by HR-APCI-TOF mass spectrum at *m/z* = 500.1390 [**15**–OCH_3]$^+$. The ^{1}H NMR spectrum of **15** displayed the protons of the fused thiopyrane moiety at 8.39, 7.88, 7.53, and 7.47 ppm. The structures of **14** and **15** have both been confirmed by X-ray diffraction analysis (Figure 4).

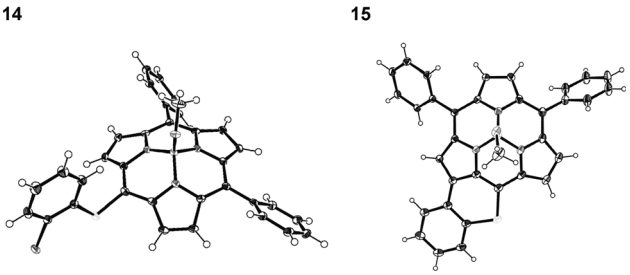

Figure 4. X-ray crystal structures of **14** (left) and **15** (right). Thermal ellipsoids are set at 50% probability level. Solvent molecules in **15** were omitted for clarity.

Crystals of **14** were obtained by slow recrystallization from a mixture of diethyl ether and hexane, whereas those of **15** were obtained by slow recrystallization from a mixture of CH_2Cl_2, methanol, and trifluoroacetic acid. Notably, the arylsulfanyl group in **14** is almost perpendicular to the subporphyrin core, similarly to a structural feature that was observed for *meso*-phenylsulfanyl subporphyrin **5a**. In contrast, the structure of **15** indicates that the arylsulfanyl group is coplanar with the subporphyrin core because of the fused structure. Subporphyrins **14** and **15** display similar bowl depths[15] of 1.44 and 1.45 Å, respectively.

Subporphyrin **14** exhibits a Soret-like band at 375 nm and a Q-like band at 461 nm, which is similar to *meso*-phenylsulfanyl-substituted subporphyrin **5a** that shows a Soret band at 375 nm and a Q-like band at 462 nm. Subporphyrin **14** is virtually nonfluorescent. Thiopyrane-fused subporphyrin **15** shows a red-shifted Soret-like band at 394 nm and a Q-like band at 516 nm (Figure 3c, Table 3). The large bathochromic shifts of **15**, in comparison to **5a** and **14**, are probably due to π-extension and decreased molecular symmetry. The fluorescence quantum yield of **15** (0.17) is distinctly higher than that of **5a** (0.03). This result may be important, suggesting that the fluorescence properties of subporphyrins bearing a sulfur atom can be tuned by structural rigidification caused by fused structures. In addition, subporphyrin **15** shows a Stokes shift of 860 cm^{-1}, which is smaller than that of **5a** (1700 cm^{-1}), in line with its rigid structure.

Conclusion

meso-Halosubporphyrins underwent S_NAr reactions with nucleophiles such as arylamines, diarylamines, thiophenols, *n*-butylthiol, phenols, ethanol, pyrrole, indole, and carbazole, under basic conditions to give corresponding A_2B-type *meso*-substituted subporphyrins in moderate to good yields. As an application of the S_NAr reactions, a thiopyrane-fused subporphyrin was synthesized, which exhibited a higher fluorescence quantum yield than its non-fused reference molecule. Exploration of novel functionalized subporphyrins by utilizing S_NAr reactions is currently underway in our laboratory.

Experimental Section

General: All reactions were performed under N_2 atmosphere. All reagents and solvents were of commercial reagent grade and were used without further purification unless where noted. 1,4-Dioxane was purified by passing through neutral alumina under nitrogen atmosphere. NBS was recrystallized from hot water before use. ^1H, ^{11}B, and ^{13}C NMR spectra were recorded on a JEOL delta-ECA600 spectrometer, and chemical shifts (δ) were reported in ppm relative to internal standards $CHCl_3$ ($\delta = 7.26$ ppm for ^1H, 77.16 ppm for ^{13}C), DMSO ($\delta = 2.50$ ppm for ^1H), 1,1,2,2-tetrachloroethane ($\delta = 6.00$ ppm for ^1H), or an external standard, $BF_3{\cdot}OEt_2$ in $CDCl_3$ ($\delta = 0.00$ ppm for ^{11}B). Spectroscopic grade solvents were used for all spectroscopic studies without further purification. UV/Vis absorption spectra were recorded on a Shimadzu UV-3600 spectrometer. Fluorescence spectra were recorded on a Shimadzu RD-5300PC spectrometer. Absolute fluorescence quantum yields were determined on HAMAMATSU C9920–02S. HR-APCI-TOF-MS spectra were recorded on a Bruker Daltonics micrOTOF LC instrument using positive-ion mode. Preparative separations were performed by silica gel chromatography (Wako gel C-300) and GPC (Bio-Beads SX-1).

Methoxo(5-chloro-10,15-diphenylsubporphyrinato)boron(III) (2b): A solution of *meso*-free subporphyrin **1** (103 mg, 242 μmol) and NCS (32.5 mg, 243 μmol, 1.0 equiv) in $CHCl_3$ (100 mL) was stirred at 60 °C for 12 h. After 12 h, the reaction mixture was poured onto water and extracted with CH_2Cl_2 (30 mL×3) and then dried with Na_2SO_4. The solvents were removed under reduced pressure. The residue was dissolved in a mixture of CH_2Cl_2 and MeOH (15 mL each) , then heated at 50 °C for 10 min. The crude product was purified by silica gel column chromatography (eluent: CH_2Cl_2/hexane/Et_2O = 1:8:1). The first yellow fraction emitting green fluorescence was collected and recrystallized from CH_2Cl_2/MeOH to give **2b** as an orange solid (66.5 mg, 145 μmol, 60%). The second fraction emitting green fluorescence was **1**. ^1H NMR (600 MHz, $CDCl_3$) $\delta = 8.25$ (d, $J = 4.6$ Hz, 2H; β), 8.10 (s, 2H; β), 8.04 (d, $J = 4.6$ Hz, 2H; β), 8.02 (d, $J = 7.8$ Hz, 4H; *meso*-Ph-*ortho*), 7.69 (t, $J = 7.6$ Hz, 4H; *meso*-Ph-*meta*), 7,62 (t, $J = 7.6$ Hz, 2H; *meso*-Ph-*para*), 0.87 ppm (s, 3H; axial OCH_3); ^{13}C NMR (150 MHz, $CDCl_3$): $\delta =$ 141.8, 141.7, 141.1, 136.9, 133.3, 128.8, 128.1, 122.8, 122.4, 121.3, 120.3, 47.0 ppm; ^{11}B NMR (193 MHz, $CDCl_3$) $\delta = -15.1$ ppm (s); UV/Vis absorption (CH_2Cl_2): λ_{max} (ε) = 370 (152000), 458 (13000), 484 nm (7000 $M^{-1}cm^{-1}$); fluorescence (CH_2Cl_2): $\lambda_{ex} = 370$ nm; $\lambda_{max} =$ 509 nm ($\Phi_f = 0.03$); HRMS (APCI-TOF, positive mode): *m/z* calcd for $C_{27}H_{16}{}^{11}B_1{}^{35}ClN_3$: 428.1125 $[M–OCH_3]^+$; found: 428.1123.

Methoxo[5,10-diphenyl-15-diphenylaminosubporphyrinato)-boron(III) (9a): In a dried 10 mL Schlenk tube, subporphyrin **2a** (19.3 mg, 38.3 μmol), diphenylamine (42.1 mg, 249 μmol, 6.5 equiv) and *t*BuOK (29.9 mg, 266 μmol, 7.0 equiv) were charged and the tube was purged with N_2. Then, dioxane (4.0 mL) was added and the resulting mixture was stirred at room temperature. After 10 min, the reaction mixture was poured onto water and extracted with CH_2Cl_2 (15 mL×3) and then dried over Na_2SO_4. The solvents were removed under reduced pressure. The residue was dissolved in a mixture of CH_2Cl_2 and MeOH (5 mL each) then heated at 50 °C for 10 min. The crude product was purified by silica gel column chromatography (eluent: CH_2Cl_2/hexane/Et_2O = 1:5:1 with 1% of MeOH). The fraction emitting orange fluorescence was collected and recrystallized from MeOH to give **9a** as a red solid (16.4 mg, 27.7 μmol, 72%). ^1H NMR (600 MHz, $CDCl_3$): $\delta = 8.03$ (s, 2H; β), 7.99 (d, $J = 7.5$ Hz, 4H; *meso*-Ph-*ortho*), 7.77 (d, $J = 4.6$ Hz, 2H; β), 7.65 (t, $J = 7.5$ Hz, 4H; *meso*-Ph-*meta*), 7.56 (t, $J = 7.5$ Hz, 2H; *meso*-Ph-*para*), 7.48 (d, $J = 4.6$ Hz, 2H; β), 7.24 (m, 8H; *meso*-NPh_2-*ortho, meta*), 7.03 (m, 2H; *meso*-NPh_2-*para*), 1.03 ppm (s, 3H; axial OCH_3); ^{11}B NMR (193 MHz, $CDCl_3$) $\delta = -14.7$ ppm (s); UV/Vis absorption (CH_2Cl_2): λ_{max} (ε) = 357 (54000), 403 (65000), 530 nm (15000 $M^{-1}cm^{-1}$); fluorescence (CH_2Cl_2): $\lambda_{ex} = 403$ nm; $\lambda_{max} =$ 587 nm ($\Phi_f = 0.39$); HRMS (APCI-TOF, positive mode): *m/z* calcd for $C_{40}H_{29}{}^{11}B_1N_4O_1$: 561.2252 $[M–OCH_3]^+$; found: 561.2258: Subporphyrins **3**–**12** were synthesized in a similar manner.

Methoxo[5,10-diphenyl-15-bis(4-methoxyphenyl)aminosubporphyrinato]boron(III) (9b): According to the general procedure, **9b** was prepared from **2a** (21.7 mg, 43.0 μmol), bis(4-methoxyphenyl)amine (47.2 mg, 206 μmol, 5 equiv) and *t*BuOK (23.8 mg, 212 μmol, 5 equiv) in dioxane (4.0 mL). The reaction took 5 min at room temperature. The crude product was purified by silica gel column chromatography (eluent: CH_2Cl_2/hexane/Et_2O = 1:4:1 with 1% of MeOH). The fraction emitting orange fluorescence was collected and recrystallized from MeOH to give **9b** as a red solid (22.6 mg, 34.6 μmol, 80%). ^1H NMR (600 MHz, $CDCl_3$): $\delta = 7.99$ (m, 6H; *meso*-Ph-*ortho*, β), 7.71 (d, $J = 4.6$ Hz, 2H; β), 7.64 (t, $J = 7.6$ Hz,

4H; *meso*-Ph-*meta*), 7.55 (t, $J=7.6$ Hz, 2H; *meso*-Ph-*para*), 7.34 (d, $J=4.6$ Hz, 2H; β), 7.25 (d, $J=8.7$ Hz, 4H; *meso*-NAr_2), 6.84 (d, $J=8.7$ Hz, 4H; *meso*-NAr_2), 3.81 (s, 6H; Ar–OCH_3), 1.09 ppm (s, 3H; axial OCH_3); ^{11}B NMR (193 MHz, $CDCl_3$) $\delta=-15.4$ ppm (s); UV/Vis absorption (CH_2Cl_2): $\lambda_{max}(\varepsilon)=359$ (65000), 408 (53000), 553 nm (21000 $M^{-1}cm^{-1}$); fluorescence (CH_2Cl_2): $\lambda_{ex}=408$ nm; $\lambda_{max}=643$ nm ($\Phi_f=0.14$); HRMS (APCI-TOF, positive mode): *m/z* calcd for $C_{41}H_{30}{}^{11}B_1N_4O_2$: 621.2463 [*M*–$OCH_3$]$^+$; found: 621.2422.

Methoxo[5,10-diphenyl-15-bis(4-dimethylaminophenyl)aminosubporphyrinato]boron(III) (9c): According to the general procedure, **9c** was prepared from **2a** (38.5 mg, 76.4 μmol), bis(4-dimethylaminophenyl)amine (82.9 mg, 325 μmol, 4.2 equiv) and *t*BuOK (34.2 mg, 30.5 μmol, 4.0 equiv) in dioxane (4.0 mL). The reaction took 10 min at room temperature. The crude product was purified by silica gel column chromatography (eluent: CH_2Cl_2/hexane/Et_2O=1:6:1 with 1% of MeOH) and GPC column chromatography. The blue fraction was collected and recrystallized from MeOH to give **9c** as a purple solid (23.8 mg, 35.1 μmol, 46%). ^1H NMR (600 MHz, $CDCl_3$) $\delta=7.98$ (d, $J=7.5$ Hz, 4H; *meso*-Ph-*ortho*), 7.93 (s, 2H; β), 7.62 (*t*, $J=7.5$ Hz, 6H; 4H for *meso*-Ph-*meta*, 2H for β), 7.52 (t, $J=7.5$ Hz, 2H; *meso*-Ph-*para*), 7.28 (m, 4H; *meso*-*N*-Ar), 7.22 (d, $J=4.6$ Hz, 2H; β), 6.71 (d, $J=8.8$ Hz, 4H; *meso*-*N*-Ar), 2.97 (s, 12H; NMe_2), 1.17 ppm (s, 3H; axial OCH_3); ^{11}B NMR (193 MHz, $CDCl_3$) $\delta=-15.0$ ppm (s); UV/Vis absorption (CH_2Cl_2): λ_{max} (ε)=364 (75000), 415 (28000), 574 nm (18000 $M^{-1}cm^{-1}$); fluorescence (CH_2Cl_2): $\lambda_{ex}=415$ nm ($\Phi_f<0.01$); HRMS (APCI-TOF, positive mode): *m/z* calcd for $C_{43}H_{36}{}^{11}B_1N_6$: 647.3096 [*M*–$OCH_3$]$^+$; found 647.3089.

Methoxo[5,10-diphenyl-15-bis(4-nitrodiphenyl)aminosubporphyrinato]boron(III) (9d): According to the general procedure, **9d** was prepared from **2b** (21.6 mg, 42.8 μmol), bis(4-nitrophenyl)-amine (19.8 mg, 76.4 μmol, 1.8 equiv) and *t*BuOK (7.1 mg, 63.2 μmol, 1.5 equiv) in DMSO (2.0 mL). The reaction took 24 h at 140 °C. The crude product was purified by silica gel column chromatography (eluent: CH_2Cl_2/hexane/Et_2O=1:6:1). The orange fraction was collected and recrystallized from MeOH to give **9d** as a red solid (13.2 mg, 19.3 μmol, 41%). ^1H NMR (600 MHz, [D_6]DMSO) $\delta=8.21$ (s, 2H; β), 8,17 (d, $J=9.1$ Hz, 4H; *meso*-NAr_2), 8.09 (d, $J=4.6$ Hz, 2H; β), 8.08 (d, $J=7.6$ Hz, 4H; *meso*-Ph-*ortho*), 7.85 (d, $J=4.6$ Hz, 2H; β), 7.78 (t, $J=7.6$ Hz, 4H; *meso*-Ph-*meta*), 7.69 (t, $J=7.6$ Hz, 2H; *meso*-Ph-*para*), 7.32 (broad s, 4H; *meso*-NAr_2), 0.75 ppm (s, 3H; axial OCH_3); ^{11}B NMR (193 MHz, $CDCl_3$) $\delta=-15.1$ ppm (s); UV/Vis absorption (CH_2Cl_2): λ_{max} (ε)=390 (88000), 501 nm (12000 $M^{-1}cm^{-1}$); fluorescence (CH_2Cl_2): $\lambda_{ex}=390$ nm ($\Phi_f<0.01$); HRMS (APCI-TOF, positive mode): *m/z* calcd for $C_{39}H_{24}{}^{11}B_1N_6O_4$: 651.1953 [*M*–$OCH_3$]$^+$; found: 651.1960.

Methoxo(5,10-diphenyl-15-*N*-pyrrolylsubporphyrinato)boron(III) (10): According to the general procedure, **10** was prepared from **2a** (40.7 mg, 80.7 μmol), pyrrole (28 μL, 400 μmol, 5 equiv) and NaH 60% dispersion on mineral oil (16 mg, 400 μmol, 5 equiv) in DMF (4.0 mL). The reaction took 30 min at room temperature. The crude product was purified by silica gel column chromatography (eluent: CH_2Cl_2/hexane/Et_2O=1:6:1). The yellow fraction emitting green fluorescence was collected and recrystallized from MeOH to give **10** as an orange solid (9.5 mg, 19.4 μmol, 24%). ^1H NMR (600 MHz, $CDCl_3$) $\delta=8.14$ (d, 2H; β), 8.12 (d, $J=4.6$ Hz, 2H; β), 8.09 (d, $J=4.6$ Hz, 2H; β), 8.05 (d, $J=7.7$ Hz, 4H; *meso*-Ph-*ortho*), 7.71 (t, $J=7.7$ Hz, 4H; *meso*-Ph-*meta*), 7.63 (t, $J=7.7$ Hz, 2H; *meso*-Ph-*para*), 7.59 (t, $J=2.2$ Hz, 2H; *meso*-pyrrole), 6.65 (t, $J=2.2$ Hz, 2H; *meso*-pyrrole), 0.88 ppm (s, 3H; axial OCH_3); ^{11}B NMR (193 MHz, $CDCl_3$) $\delta=-15.2$ ppm (s); UV/Vis absorption (CH_2Cl_2): λ_{max} (ε)=373 (142000), 459 (9000), 489 nm (8000 $M^{-1}cm^{-1}$); fluorescence (CH_2Cl_2): $\lambda_{ex}=373$ nm; $\lambda_{max}=523$ nm ($\Phi_f=0.14$); HRMS (APCI-TOF, positive mode): *m/z* calcd for $C_{31}H_{20}{}^{11}B_1N_4$: 459.1781 [*M*–$OCH_3$]$^+$; found: 459.1779.

Methoxo(5,10-diphenyl-15-*N*-indolylsubporphyrinato)boron(III) (11): According to the general procedure, **11** was prepared from **2a** (22.0 mg, 43.6 μmol), indole (25.5 mg, 218 μmol, 5 equiv), and KO*t*Bu (27.2 mg, 223 μmol, 5 equiv) in dioxane (4.0 mL). The reaction took 2 h at room temperature. The crude product was purified by silica gel column chromatography (eluent: CH_2Cl_2/hexane/Et_2O=1:6:1). The yellow fraction bearing green fluorescence was collected and recrystallized from MeOH to give **11** as an orange solid (15.6 mg, 28.9 μmol, 66%). ^1H NMR (600 MHz, $CDCl_3$, −40 °C) $\delta=8.37$ (d, $J=3.6$ Hz. 1H; *meso*-indolyl), 8.21 (s, 1H; β), 8.19 (d, $J=8.3$ Hz, 1H; *meso*-indolyl), 8.17 (s, 1H; β), 8.09 (m, 6H; 4H for *meso*-Ph-ortho, 2H for β), 7.95 (d, $J=3.6$ Hz, 2H; β), 7.91 (d, $J=7.8$ Hz, 1H; *meso*-indolyl), 7.83 (d, $J=7.8$ Hz, 1H; *meso*-indolyl), 7.82 (d, $J=4.6$ Hz, 2H; β), 7.72 (m, 4H; *meso*-Ph-*meta*), 7.64 (m, 2H; *meso*-Ph-*para*), 7.23 (t, $J=7.3$ Hz, 1H; *meso*-indolyl), 7,41 (d, $J=3.2$ Hz, 1H; *meso*-indolyl), 7.38 (t, $J=7.2$ Hz, 1H; *meso*-indolyl), 7.16 (t, $J=7.2$ Hz, 1H; *meso*-indolyl), 7.04 (d, $J=2.3$ Hz, 1H; *meso*-indolyl), 6.94 (d, $J=2.3$ Hz, 1H; *meso*-indolyl), 6.85 (t, $J=7.2$ Hz, 1H; *meso*-indolyl), 6.27 (d, $J=8.4$ Hz, 1H; *meso*-indolyl), 1.00 (s, 3H; axial OCH_3), 0.89 ppm (s, 3H; axial OCH_3); ^{11}B NMR (193 MHz, $CDCl_3$, −40 °C) $\delta=-15.1$ ppm (s), −15.2 (s); UV/Vis absorption (CH_2Cl_2): λ_{max} (ε)=374 (129000), 459 (12000), 489 nm (9000 $M^{-1}cm^{-1}$); fluorescence (CH_2Cl_2): $\lambda_{ex}=374$ nm; $\lambda_{max}=528$ nm ($\Phi_f=0.15$); HRMS (APCI-TOF, positive mode): *m/z* calcd for $C_{35}H_{22}{}^{11}B_1N_4$: 509.1938 [*M*–$OCH_3$]$^+$; found: 509.1945.

Methoxo(5,10-diphenyl-15-*N*-carbazolylsubporphyrinato)-boron(III) (12): According to the general procedure, **12** was prepared from **2a** (20.5 mg, 40.7 μmol), carbazole (34.3 mg, 205 μmol, 5 equiv), and KO*t*Bu (24.2 mg, 216 μmol, 5 equiv) in dioxane (4.0 mL). The reaction took 30 min at 60 °C. The crude product was purified by silica gel column chromatography (eluent: CH_2Cl_2/hexane/Et_2O=1:5:1). The yellow fraction emitting green fluorescence was collected and recrystallized from MeOH to give **12** as an orange solid (20.1 mg, 34.0 μmol, 84%). ^1H NMR (600 MHz, $CDCl_3$) $\delta=8.35$ (d, $J=7.6$ Hz, 1H; *meso*-carbazole), 8.27 (d, $J=7.8$ Hz, 1H; *meso*-carbazole), 8.18 (s, 2H; β), 8.08 (d, $J=6.8$ Hz, 4H; *meso*-Ph-*ortho*), 8.01 (d, $J=4.6$ Hz, 2H; β), 7.91 (d, $J=8.5$ Hz, 1H; *meso*-carbazole), 7.71 (t, $J=7.6$ Hz, 4H; *meso*-Ph-*meta*), 7.67 (d, $J=4.6$ Hz, 2H; β), 7.63 (t, $J=7.6$ Hz, 2H; *meso*-Ph-*para*), 7.67 (t, $J=7.8$ Hz, 1H; *meso*-carbazole), 7.47 (t, $J=7.6$ Hz, 1H; *meso*-carbazole), 7.26 (t, $J=7.6$ Hz, 1H; *meso*-carbazole), 7.01 (t, $J=7.8$ Hz, 1H; *meso*-carbazole), 6.11 (d, $J=8.5$ Hz, 2H; *meso*-carbazole), 1.06 ppm (s, 3H; axial OCH_3); ^{11}B NMR (193 MHz, $CDCl_3$) $\delta=-15.0$ ppm (s); UV/Vis (CH_2Cl_2): λ_{max} (ε)=376 (111000), 459 (10000), 483 nm (5000 $M^{-1}cm^{-1}$); fluorescence (CH_2Cl_2): $\lambda_{ex}=376$ nm; $\lambda_{max}=531$ nm ($\Phi_f=0.15$); HRMS (APCI-TOF, positive mode): *m/z* calcd for $C_{39}H_{24}{}^{11}B_1N_4$: 590.2279 [M]$^+$; found: 590.2282.

Methoxo(5,10-diphenyl-15-(2-bromophenylthio)subporphyrinato)boron(III) (14): In a 20 mL round bottom flask were placed **2a** (31.2 mg, 61.8 μmol) and cesium carbonate (188 mg, 577 μmol). Dioxane (5.0 mL) and 2-bromobenzenethiol (36 μL, ca. 2.5 equiv) were added in this order and the resulting solution was heated at 60 °C. After 9.5 h, the reaction was quenched with water and extracted with CH_2Cl_2. Organic layer was collected and dried over Na_2SO_4. After evaporation of the solvent, crude product was purified by silica gel column chromatography (eluent: CH_2Cl_2/hexane/ether=1:5:1). Yellow fraction was collected and recrystallized from MeOH to give **14** as an orange solid (29.3 mg, 47.8 μmol, 77%). ^1H NMR (600 MHz, $CDCl_3$) $\delta=8.28$ (d, $J=4.6$ Hz, 2H; *β*), 8.12 (s, 2H; β), 8.07 (d, $J=4.6$, 2H; β), 8.04 (d, $J=6.8$ Hz, 4H; *meso*-Ph-*ortho*), 7.70 (t, $J=7.6$ Hz, 4H; *meso*-Ph-*meta*), 7.63 (m, 3H; 2H for *meso*-Ph-

para, 1H for *meso*-SAr), 6.94 (t, $J=6.4$ Hz, 1H; *meso*-SAr), 6.86 (t, $J=6.9$ Hz, 1H; *meso*-SAr), 6.65 (d, $J=7.7$ Hz, 1H; *meso*-SAr), 0.90 ppm (s, 3H; axial OCH_3); ^{11}B NMR (193 MHz, $CDCl_3$) $\delta=-15.1$ ppm (s); UV/Vis absorption (CH_2Cl_2): λ_{max} (ε) = 375 (120000), 461 nm (11000 $M^{-1}cm^{-1}$); fluorescence (CH_2Cl_2): $\lambda_{ex}=375$ nm ($\Phi_f < 0.01$); HRMS (APCI-TOF, positive mode): *m/z* calcd for $C_{33}H_{20}{}^{11}B_1N_3S^{79}Br$: 580.0655 $[M-OCH_3]^+$; found: 580.0659.

Thiopyrane-fused subporphyrin 15: In a dried 10 mL Schlenk tube, subporphyrin **14** (10.4 mg, 17.0 μmol), $Pd(OAc)_2$ (2.5 mg, 11 μmol, 65 mol%), tBuCO$_2$H (10.5 mg, 103 μmol, 6 equiv), and K_2CO_3 (27.6 mg, 200 μmol, 12 equiv) were placed and purged with N_2. To this, DMA (1.0 mL) was added and the resulting solution was stirred at 100 °C. After 13 h, the reaction mixture was cooled and poured onto water. The organic layer was extracted with AcOEt/hexane (1:3; 20 mL×3) and the solvents were removed under reduced pressure. Crude product was purified by silica gel column chromatography (eluent = CH_2Cl_2/hexane/Et_2O = 1:8:1). An orange fraction emitting orange fluorescence was collected and recrystallized from MeOH to give **15** as a red solid (5.0 mg, 9.3 μmol, 55%). ^1H NMR (600 MHz, $CDCl_3$) $\delta=8.39$ (d, $J=6.9$ Hz, 1H; fused-SPh), 8.23 (s, 1H; β), 8.12–7.98 (m, 8H; 4H for *meso*-Ph-*ortho*, 4H for β), 7.88 (d, $J=7.8$ Hz, 1H; fused-SPh), 7.72 (t, $J=7.8$ Hz, 2H; *meso*-Ph-*meta*), 7.68 (t, $J=7.4$ Hz, 2H; *meso*-Ph-*meta*), 7.64–7.58 (m, 2H; *meso*-Ph-*para*), 7.53 (t, $J=7.6$ Hz, 1H; fused-SPh), 7,47 (t, $J=7.6$ Hz, 1H; fused-SPh), 1.04 ppm (s, 3H; axial OCH_3); ^{11}B NMR (193 MHz, $CDCl_3$) $\delta=-14.1$ ppm (s); UV/Vis absorption (CH_2Cl_2): λ_{max} (ε) = 394 (108000), 516 nm (19600 $M^{-1}cm^{-1}$); fluorescence (CH_2Cl_2): $\lambda_{ex}=394$ nm; $\lambda_{max}=548$ nm ($\Phi_f=0.17$); HRMS (APCI-TOF, positive mode): *m/z* calcd for $C_{33}H_{19}{}^{11}B_1N_3S$: 500.1393 $[M-OCH_3]^+$; found: 500.1390.

X-ray crystallographic analysis: X-ray data were recorded by using a Rigaku XtaLAB P-200 system. The structure were solved by using direct methods (SIR-97[16] or SHELXS-97[17]). Structure refinements were carries out by using SHELXL-97. CCDC 1014392 (**9a**), 1014393 (**9b**), 1014394 (**9c**), 1014395 (**10**), 1014396 (**11**), 1014397 (**12**), 1021559 (**14**), and 1021558 (**15**) contain supplementary crystallographic data for this paper. These data can be obtained free of charge from The Cambridge Crystallographic Data Center via www.ccdc.cam.ac.uk/data_request/cif.

Time-resolved fluorescence decay: A time-correlated single photon counting (TCSPC) system was used for measurements of spontaneous fluorescence decay. As an excitation light source, we used a mode-locked Ti:sapphire laser (MaiTai BB, Spectra Physics) which provides ultrashort pulse (80 fs at full width half maximum, fwhm) with high repetition rate (80 MHz). This high repetition rate slows down to 1 M ~800 kHz by using a homemade pulse-picker. The pulse-picked output pulse was frequency-doubled by a 1 mm thickness of a BBO crystal (EKSMA). The fluorescence was collected by a microchannel plate photomultiplier (MCP-PMT, R3809U-51, Hamamatsu) with a thermoelectric cooler (C4748, Hamamatsu) connected to a TCSPC board (SPC-130, Becker & Hickel GmbH). The overall instrumental response function was about 25 ps (fwhm).

Acknowledgements

The work at Kyoto was supported by JSPS KAKENHI Grant Numbers No. 25220802 and 25620031. H.N. and M.K. acknowledge a JSPS Fellowship for Young Scientists. The work at Yonsei was supported by the Global Research Laboratory (2013K1A1A2A02050183) through the National Research Foundation of Korea (NRF) funded by the Ministry of Science, ICT (Information and Communication Technologies) and Future Planning.

Keywords: fluorescence · fusion reactions · nucleophilic aromatic substitution · porphyrinoids · subporphyrins

[1] a) T. Torres, *Angew. Chem. Int. Ed.* **2006**, *45*, 2834; *Angew. Chem.* **2006**, *118*, 2900; b) Y. Inokuma, A. Osuka, *Dalton Trans.* **2008**, 2517; c) A. Osuka, E. Tsurumaki, T. Tanaka, *Bull. Chem. Soc. Jpn.* **2011**, *84*, 679; d) C. G. Claessens, D. González-Rodríguez, M. S. Rodríguez-Morgade, A. Medina, T. Torres, *Chem. Rev.* **2014**, *114*, 2192.

[2] a) R. Myśliborski, L. Latos-Grażyński, L. Szterenberg, T. Lis, *Angew. Chem. Int. Ed.* **2006**, *45*, 3670; *Angew. Chem.* **2006**, *118*, 3752; b) Z.-L. Xue, Z. Shen, J. Mack, D. Kuzuhara, H. Yamada, T. Okujima, N. Ono, X.-Z. You, N. Kobayashi, *J. Am. Chem. Soc.* **2008**, *130*, 16478; c) D. Kuzuhara, H. Yamada, Z.-L. Xue, T. Okujima, S. Mori, Z. Shen, H. Uno, *Chem. Commun.* **2011**, *47*, 722.

[3] Y. Inokuma, J. H. Kwon, T. K. Ahn, M.-C. Yoo, D. Kim, A. Osuka, *Angew. Chem. Int. Ed.* **2006**, *45*, 961; *Angew. Chem.* **2006**, *118*, 975.

[4] a) N. Kobayashi, Y. Takeuchi, A. Matsuda, *Angew. Chem. Int. Ed.* **2007**, *46*, 758; *Angew. Chem.* **2007**, *119*, 772; b) Y. Inokuma, Z. S. Yoon, D. Kim, A. Osuka, *J. Am. Chem. Soc.* **2007**, *129*, 4747; c) Y. Takeuchi, A. Matsuda, N. Kobayashi, *J. Am. Chem. Soc.* **2007**, *129*, 8271; d) S. Zhao, C. Liu, Y. Guo, J.-C. Xiao, Q.-Y. Chen, *Synthesis* **2014**, *46*, 1674.

[5] a) Y. Inokuma, S. Easwaramoorthi, S. Y. Jang, K. S. Kim, D. Kim, A. Osuka, *Angew. Chem. Int. Ed.* **2008**, *47*, 4840; *Angew. Chem.* **2008**, *120*, 4918; b) S. Hayashi, Y. Inokuma, A. Osuka, *Org. Lett.* **2010**, *12*, 4148; c) Y. Inokuma, S. Easwaramoorthi, Z. S. Yoon, D. Kim, A. Osuka, *J. Am. Chem. Soc.* **2008**, *130*, 12234.

[6] M. Kitano, S. Hayashi, T. Tanaka, H. Yorimitsu, N. Aratani, A. Osuka, *Angew. Chem. Int. Ed.* **2012**, *51*, 5593; *Angew. Chem.* **2012**, *124*, 5691.

[7] a) M. Kitano, S. Hayashi, T. Tanaka, N. Aratani, A. Osuka, *Chem. Eur. J.* **2012**, *18*, 8929; b) W.-Y. Cha, J. M. Lim, K. H. Park, M. Kitano, A. Osuka, D. Kim, *Chem. Commun.* **2014**, *50*, 8491; c) M. Kitano, D. Shimizu, T. Tanaka, H. Yorimitsu, A. Osuka, *J. Por. Phthal.* **2014**, ##in press.

[8] M. Kitano, J. Sung, K. H. Park, H. Yorimitsu, D. Kim, A. Osuka, *Chem. Eur. J.* **2013**, *19*, 16523.

[9] L.-C. Gong, D. Dolphin, *Can. J. Chem.* **1985**, *63*, 406.

[10] a) M. J. Crossley, L. G. King, S. M. Pyke, *Tetrahedron* **1987**, *43*, 4569; b) M. J. Crossley, J. J. Gosper, L. G. King, *Tetrahedron Lett.* **1988**, *29*, 1597.

[11] a) M. C. Balaban, A. Eichhöfer, G. Buth, R. Hauschild, J. Szmytkowski, H. Kalt, T. S. Balaban, *J. Phys. Chem. A J. Phys. Chem. B.* **2008**, *112*, 5512; b) A. M. V. M. Pereira, C. M. A. Alonso, M. G. P. M. S. Neves, A. C. Tomé, A. M. S. Silva, F. A. A. Paz, J. A. S. Cavaleiro, *J. Org. Chem.* **2008**, *73*, 7353; c) K. Yamashita, K. Kataoka, M. S. Asano, K. Sugiura, *Org. Lett.* **2012**, *14*, 190; d) A. A. Ryan, S. Plunkett, A. Casey, T. McCabe, M. O. Senge, *Chem. Commun.* **2014**, *50*, 353; e) C. H. Devillers, S. Hebié, D. Lucas, H. Cattey, S. Clément, S. Richter, *J. Org. Chem.* **2014**, *79*, 6424.

[12] a) Q. Chen, Y.-Z. Zhu, Q.-J. Fan, S.-C. Zhang, J.-Y. Zheng, *Org. Lett.* **2014**, *16*, 1590.

[13] a) Y. Liu, H. Lin, J. T. Dy, K. Tamaki, J. Nakazaki, D. Nakayama, S. Uchida, T. Kubo, H. Segawa, *Chem. Commun.* **2011**, *47*, 4010; b) Y. Liu, H. Lin, J. Li, J. T. Dy, K. Tamaki, J. Nakazaki, D. Nakayama, C. Nishiyama, S. Uchida, T. Kubo, H. Segawa, *Phys. Chem. Chem. Phys.* **2012**, *14*, 16703; c) L. Favereau, J. Warnan, F. B. Anne, Y. Pellegrin, E. Blart, D. Jacquemin, F. Odobel, *J. Mater. Chem. A* **2013**, *1*, 7572; d) Y. Liu, H. Lin, J. T. Dy, K. Tamaki, J. Nakazaki, C. Nishiyama, S. Uchida, T. Kubo, H. Segawa, J. Li, *J. Phys. Chem. C* **2014**, *118*, 1426; e) J. Haumesser, A. M. V. M. Pereira, J.-P. Gisselbrecht, K. Merahi, S. Choua, J. Weiss, J. A. S. Cavaleiro, R. Ruppert, *Org. Lett.* **2013**, *15*, 6282.

[14] a) Y. Kawamata, S. Tokuji, H. Yorimitsu, A. Osuka, *Angew. Chem. Int. Ed.* **2011**, *50*, 8867; *Angew. Chem.* **2011**, *123*, 9029; b) Y. Yamamoto, S. Tokuji, T. Tanaka, H. Yorimitsu, A. Osuka, *Asian J. Org. Chem.* **2013**, *2*, 320; c) Y. Yamamoto, S. Tokuji, T. Tanaka, H. Yorimitsu, A. Osuka, *Heterocycles* **2014**, *88*, 231; d) H. Yorimitsu, A. Osuka, *Asian J. Org. Chem.* **2013**, *2*, 356.

[15] Bowl depth is defined as the distance from the mean plane of the peripheral six β-carbons to the center boron atom.

[16] A. Altomare, M. C. Burla, M. Camalli, G. L. Cascarano, C. Giaco-vazzo, A. Guagliardi, A. G. G. Moliterni, G. Polidori, R. Spagna, *J. Appl. Crystallogr.* **1999**, *32*, 115.

[17] SHELXL-97 and SHELXS-97, Program for the Refinement of Crystal Structures from Diffraction Data, University of Göttingen, Göttingen (Germany); G. M. Sheldrick, T. R. Schneider, *Methods Enzymol.* **1997**, *277*, 319.

Received: September 3, 2014
Published online on ■■ ■■, 0000

FULL PAPER

Porphyrinoids

D. Shimizu, H. Mori, M. Kitano, W.-Y. Cha, J. Oh, T. Tanaka, D. Kim, A. Osuka**

■■ – ■■

Nucleophilic Aromatic Substitution Reactions of *meso*-Bromosubporphyrin: Synthesis of a Thiopyrane-Fused Subporphyrin

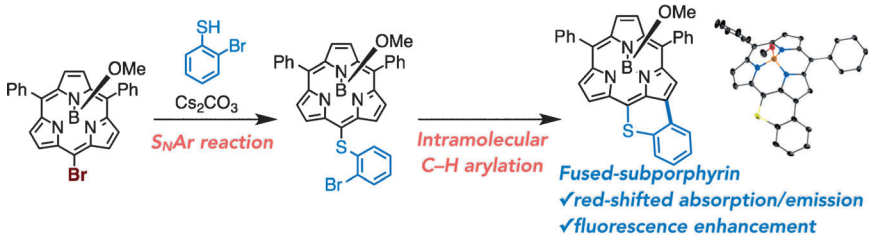

Shine like a S_NAr: *meso*-Bromosubporphyrin undergoes nucleophilic aromatic substitution (S_NAr) reactions with a variety of heteroatom nucleophiles, such as arylamines, diarylamines, phenols, ethanol, thiophenols, *n*-butanethiol, pyrrole, indole and carbazole, in the presence of suitable bases to provide the substitution products. The S_NAr reaction with 2-bromothiophenol and subsequent intramolecular arylation reaction affords a thiopyrane-fused subporphyrin.